Multiple and weak-coupling charge-density-wave transitions in $Y_5Ir_4Si_{10}$

Y. K. Kuo* and Y. Y. Chen
Department of Physics, National Dong Hwa University, Hualien 97401, Taiwan

L. M. Wang
Department of Electrical Engineering, Da-Yeh University, Chang-Hwa 515, Taiwan

H. D. Yang†
Department of Physics, National Sun-Yat-Sen University, Kaohsiung 804, Taiwan
(Received 25 February 2004; published 30 June 2004)

Physical characterizations on the ternary compound $Y_5Ir_4Si_{10}$ by using electrical resistivity (ρ), Hall coefficient (R_H), magnetic susceptibility (χ), specific heat (C_P), thermal conductivity (κ), and thermoelectric power are reported. For all measured transport and thermodynamic properties, successive anomalies due to charge-density-wave (CDW) formation were observed. In contrast to the strong-coupled nature of the phase transitions found in the isostructural compounds $R_5Ir_4Si_{10}$ (R=Dy-Lu), $Y_5Ir_4Si_{10}$ could be described as a weak-coupled CDW system. Most interestingly, the complex temperature-dependent thermoelectric power and sign reversal of Hall coefficient in this material indicate a drastic modification of Fermi surface and a sudden change of the band structure, associated with the electron-hole asymmetry at the transitions.

DOI: 10.1103/PhysRevB.69.235114 PACS number(s): 71.45.Lr, 71.20.Lp, 65.40.−b

I. INTRODUCTION

Observations on the coexistence of superconductivity and charge-density-wave (CDW) ground state are well documented for many low-dimensional systems.[1] However, this phenomenon is rarely seen in three-dimensional (3D) materials. Recently, ternary rare-earth transition-metal silicides $R_5T_4Si_{10}$ (R=rare-earth elements; T=Co, Ir, Rh, and Os), crystallize in the 3D tetragonal $Sc_5Co_4Si_{10}$-type structure, have attracted a considerable attention due to the indication of the coexistence of superconductivity and CDW formation. In addition, the interplay between superconductivity and long-range magnetic ordering at low temperatures (below 10 K) in these materials has been studied in detail.[2–14] For instances, superconducting transitions at T_C=8.2, 3.8, and 2.5 K were found in $R_5Ir_4Si_{10}$ for R=Sc, Lu, and Y; and antiferromagnetic transitions at T_N=5.0, 2.0, 3.0, and 1.9 K for R=Dy, Ho, Er, and Tm, respectively.

High-temperature phase transitions attributed to the CDW formation were also found in these ternary silicides. The direct evidence of CDW formation in this class of materials was given by Becker *et al.*,[15] Galli *et al.*,[16,17] and van Smaalen.[18] Here the CDW superlattices in single crystal x-ray diffraction were discovered in $Lu_5Ir_4Si_{10}$ and $Er_5Ir_4Si_{10}$. The results of the x-ray diffraction confirmed the existence of both incommensurate and commensurate CDW states in these compounds. For example, $Er_5Ir_4Si_{10}$ exhibits an incommensurate CDW state at T_{CDW}=155 K, which locks into a pure commensurate state below $T_{lock\text{-}in}$=55 K.[16] In addition, both $Lu_5Ir_4Si_{10}$ and $Er_5Ir_4Si_{10}$ were considered as strong-coupled CDW materials, as evidenced by the huge spike-shaped specific heat jumps at their T_{CDW}'s.[15,16] Recent studies of thermal properties and single crystal x-ray diffraction on $R_5Ir_4Si_{10}$ (R=Dy-Lu) suggested that both incommensurate CDW transition (at T_{CDW}) and lock-in (at $T_{lock\text{-}in}$) transition are expected to exist in these materials.[18,19] It was generally found that the transition temperatures decrease quasilinearly with decreasing lattice constant of rare-earth ions from Dy to Lu. Such a result indicates that the effect of ionic size play an important role to the CDW transitions in this class of materials.[19]

The ionic radius of yttrium is close to dysprosium, and slightly larger than holmium and lutetium. On the other hand, Y^{3+} is nonmagnetic with empty $4d$ electronic state, while Dy^{3+} to Yb^{3+} are magnetic with $4f$ electronic state. It would be extremely informative to examine the effects of ionic size, magnetism, as well as electronic state to the anomalous features at the CDW transitions by comparing the physical properties between $Y_5Ir_4Si_{10}$ and other isostructural compounds. In this paper, we report a detailed investigation on $Y_5Ir_4Si_{10}$ near its CDW transitions by means of electrical transport (ρ and R_H), thermodynamic (χ and C_P) and thermal transport (κ and TEP) measurements. In these measurements, successive phase transitions due to CDW formation were identified at $T_{CDW1}\sim 225$ K, $T_{CDW2}\sim 200$ K and $T_{lock\text{-}in}\sim 145$ K, respectively, and pronounced anomalous responses were observed. In particular, the very complex temperature-dependent thermoelectric power and sign reversal of the Hall coefficient in $Y_5Ir_4Si_{10}$ indicate a drastic modification of the band structure near its Fermi surface, associated with the electron-hole asymmetry at these transitions. However, the observed anomalous responses are considerably weaker than those found in the $R_5Ir_4Si_{10}$ (R=Dy, Ho, Er, Tm, and Lu) compounds. Such a result suggests that $Y_5Ir_4Si_{10}$ could be described as a weak-coupled CDW material.

II. EXPERIMENTAL DETAILS

The preparation and characterization of polycrystalline $Y_5Ir_4Si_{10}$ have been described elsewhere.[2,3] Briefly, samples were prepared by arc-melting stoichiometric mixtures of high-purity elements in a Zr-gettered argon atmosphere. The resulting ingots were turned and remelted at least five times

to promote homogeneity. Samples were then sealed in quartz ampoules with about 160 Torr of argon and annealed at 1250 °C for one day followed by three days at 1050 °C. An x-ray analysis taken with CuK radiation on powder specimens was consistent with the expected $Sc_5Co_4Si_{10}$-type structure, with no other phases present in the diffraction spectrum.

The electrical transport measurements were carried out by a six-probe technique, with a typical dimension of 2 mm in length, 1 mm in width, and 100 μm in thickness, which enables us to measure simultaneously the longitudinal resistivity and Hall voltage. The Hall voltages were measured by reversing the field direction at a fixed temperature to eliminate the offset voltage due to the unbalanced Hall terminals. The Hall coefficient measurement was taken in a magnetic field of 7 T, and a typical dc current density of 50 A/cm^2 was applied to the sample. The temperature dependence of magnetic susceptibility was obtained with a commercial superconducting quantum interference device magnetometer (Quantum Design MPMSR2) in a field of 1000 Oe. Note that the magnetic coupling to the static CDW structure in this class of materials is considered to be weak, as the measured physical properties near the CDW transition in $Lu_5Rh_4Si_{10}$ are magnetic field independent up to 8 T.[20]

Relative specific heats were performed with a high-resolution ac calorimeter, using chopped light as a heat source. Thermal conductivity and thermoelectric power measurements were carried out simultaneously in a close-cycle refrigerator from 8 to 300 K, using a direct heat-pulse technique. The details of our experimental techniques on thermal measurements can be found in Ref. 21.

III. RESULTS AND DISCUSSIONS

A. Resistivity

The temperature-dependent resistivity (ρ versus T) between 2 to 300 K of $Y_5Ir_4Si_{10}$ is shown in Fig. 1. By decreasing temperature, three noticeable kinks can be resolved at about 227, 200, and 146 K, respectively. The anomalous features are much more apparent in a $d\rho/dT$ versus. T plot, as illustrated in the inset of Fig. 1. Since the observations of CDW superlattices from the x-ray diffraction in $Ho_5Ir_4Si_{10}$, $Er_5Ir_4Si_{10}$, $Tm_5Ir_4Si_{10}$, and $Lu_5Ir_4Si_{10}$ have been provided as the direct evidence of CDW formations below T_{CDW}'s,[15–18] the nature of these phase transitions found in $Y_5Ir_4Si_{10}$ is presumably associated with the formation of CDW. We note that the resistive anomalies observed in this study are much more pronounced than that previously reported.[7,12] In particular, the phase transitions at 227 and 146 K are unambiguously identified. In the normal state (230 K $< T <$ 300 K), $\rho(T)$ decreases with lowering temperature and exhibits a metallic character. The residual resistivity ratio $\rho(300\text{ K})/\rho(4.2\text{ K})$ is estimated to be about 2.2, relatively small for a metal. At 227 and 200 K, two different CDW transitions affecting different parts of the Fermi surface occur, resulting in successive anomalous resistivity increases at these temperatures. At 146 K, a sharp decrease in ρ accompanied with a clear thermal hysteresis between 80 and 150 K was observed, as shown in Fig. 2. These features were also

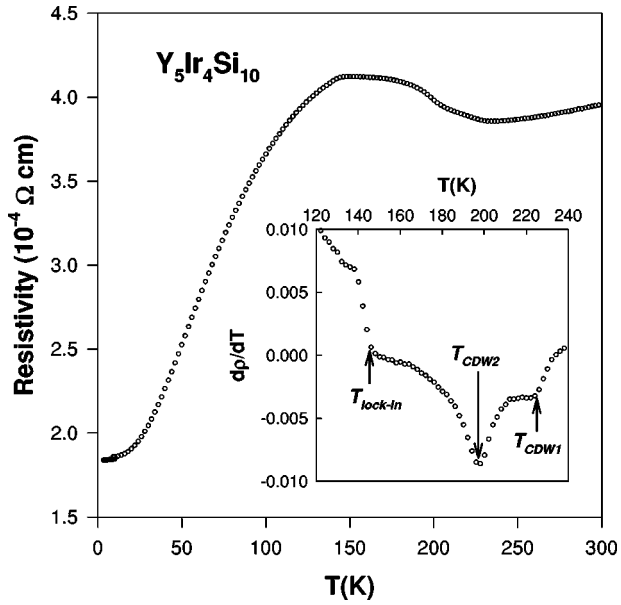

FIG. 1. Electrical resistivity as a function of temperature between 2 and 300 K for $Y_5Ir_4Si_{10}$. Three anomalies due to CDW formations are indicated by arrows in the $d\rho/dT$ versus T plot.

found in $Er_5Ir_4Si_{10}$ and $Tm_5Ir_4Si_{10}$ at 55 and 110 K, respectively, and the corresponding transitions have been identified to be a lock-in transition by single crystal x-ray diffraction experiments.[16,18] Notice that no detectable hysteresis was resolved for the upper two transitions. Such an observation suggests that the CDW transitions at 228 and 200 K are most likely second-order, while the transition at 146 K is most probably a lock-in with a first-order character. We will argue that the lock-in transition in $Y_5Ir_4Si_{10}$ leads to a partly restoration of the Fermi surface, as evidenced by the abrupt

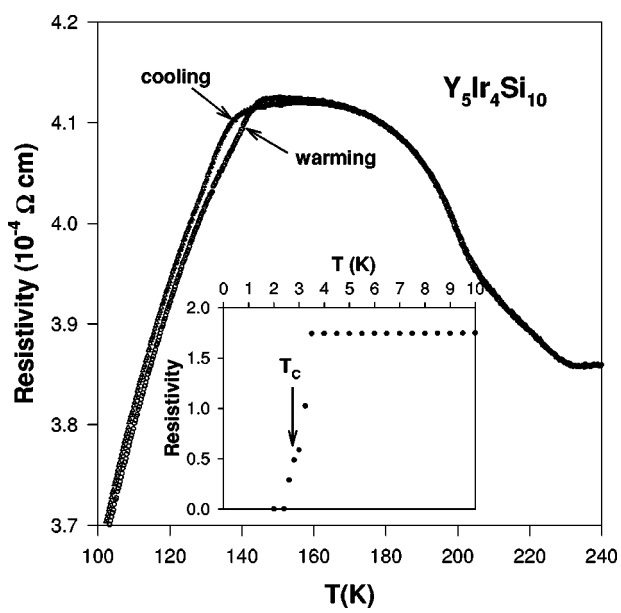

FIG. 2. The hysteresis loop between warming and cooling processes is clearly seen in ρ for $Y_5Ir_4Si_{10}$ below the lock-in transition. Inset: the sample undergoes superconducting transition at around 2.5 K.

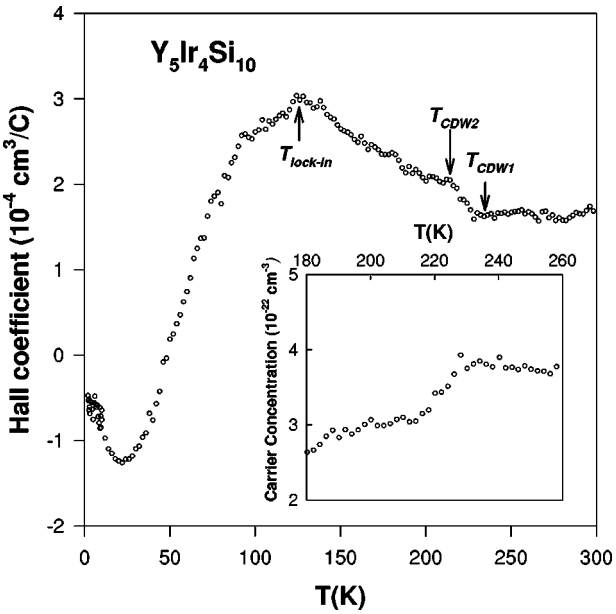

FIG. 3. Hall coefficient as a function of temperature between 2 and 300 K for $Y_5Ir_4Si_{10}$. Inset shows the decrease of carrier concentration at $T_{CDW1}=200$ K, assuming one-band model.

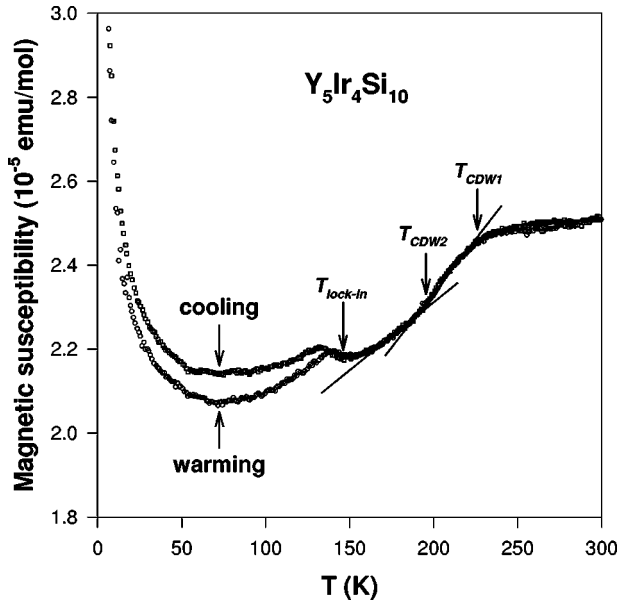

FIG. 4. The temperature (2–300 K) dependence of magnetic susceptibility for $Y_5Ir_4Si_{10}$.

decrease in resistivity below $T_{\text{lock-in}}$. Upon further cooling, the resistivity of $Y_5Ir_4Si_{10}$ continuously decreases, then develops into a plateau below 20 K, and finally goes superconducting at about 2.5 K, as shown in the inset of Fig. 2. It is noted that the transition temperatures in $Y_5Ir_4Si_{10}$ are comparable to those in $Dy_5Ir_4Si_{10}$ ($T_{CDW}=211$ K and $T_{\text{lock-in}}=165$ K),[19] as Y and Dy have nearly the same ionic size. Nevertheless, the physical properties of the CDW transitions in these two materials are rather different, as Y and Dy have different electronic states (4*d* versus 4*f*). Such a result suggests that the ionic-size effect is not only the important parameter for these phase transitions, but the electronic-configuration difference also significantly affects the physical properties in this class of materials.

B. Hall coefficient

The temperature-dependent Hall coefficient (R_H) for $Y_5Ir_4Si_{10}$ is displayed in Fig. 3. In the normal state, the R_H value is about $1.5\times10^{-4}(\text{cm}^3/\text{C})$, comparable to other CDW materials.[22,23] The positive R_H value at high temperatures signifies that hole-type carriers dominate its electrical transport. As shown in Fig. 3, an increase of the Hall coefficient is observed near $T_{CDW1}\sim230$ K, corresponding to a decrease of carrier concentration due to CDW formation (see the inset of Fig. 3). Note that here we simply apply the one-band model for the estimation of carrier concentration, where $Y_5Ir_4Si_{10}$ is expected to be two-band as the material stays conducting. Consequently, the measured Hall coefficient is an average of the hole pockets and electron pockets weighted by their mobilities. For example, a two-band model discussed by Ong on the well-studied CDW system $NbSe_3$ gave a satisfactory description of its transport properties.[24] However, the lack of the resistance anisotropy and magneto-transport measurements on single crystal of $Y_5Ir_4Si_{10}$ makes such an analysis unfeasible at this moment.

Upon further cooling, a kink in R_H at $T_{CDW2}\sim200$ K followed with a rapid decrease below $T_{\text{lock-in}}\sim140$ K, and then a sign reversal at low temperatures were observed. Notice that the anomalous feature in R_H is considerably weaker for the second CDW transition around 200 K than the first CDW transition around 230 K. Such a result indicates that the pieces of Fermi surface responsible for the electrical transport are more influenced by the first CDW formation at $T_{CDW1}\sim230$ K than the second CDW transition at $T_{CDW2}\sim200$ K. Below $T_{\text{lock-in}}\sim140$ K, a sharp reduction in R_H is observed. Such an abrupt change in R_H is attributed to the sudden change of the band structure, associated with the electron-hole asymmetry at the transition. In other words, the occurrence of the lock-in transition reduces the hole pockets but enlarges the electron pockets, leading to the compensation of charge carriers in this material. Around 50 K, the sample is fully compensated and the R_H approaches zero. Below 50 K, the Hall coefficient changes sign from positive values to negative values. The remarkable sign change of Hall coefficient was also discovered in the well-known CDW material $NbSe_2$, which is attributed to the drastic change in the electronic mean-free path or mobility induced by the transitions.[23] Notice that an upturn in R_H below 20 K was observed. The origin of this feature is not clear at this moment and deserves more investigations. The Hall coefficient data will be compared with the thermoelectric power result in later section for more discussion.

C. Magnetic susceptibility

Magnetic susceptibility (χ) as a function of temperature for $Y_5Ir_4Si_{10}$ is plotted in Fig. 4. The measured χ is roughly constant in the normal state with a value of 2.5×10^{-5} emu/mol. With lowering temperature, a successive

reduction in χ near T_{CDW1}(~230 K) and T_{CDW2}(~200 K) was observed. These transition temperatures found in the χ measurement coincide well with the increases in ρ, which are attributed to a partial opening of energy gaps and thus a loss of electronic density of states at the Fermi surface due to CDW formation. It is noted that the reduction rate in magnetic susceptibility is different at T_{CDW1} (larger slope) and T_{CDW2} (smaller slope), as indicated by straight lines in Fig. 4. With further decreasing temperature, a kink accompanied with a broad peak was found at $T_{\text{lock-in}} \sim 145$ K. Such an increase in χ corresponds well to the decrease in ρ at the lock-in transition, in accordance with the aforementioned partly restoration of the Fermi surface at $T_{\text{lock-in}}$. The low-T Curie-like tail is presumably due to the presence of a small amount of paramagnetic impurities in the sample. Besides, an obvious thermal hysteresis loop between heating and cooling cycles was seen in χ below $T_{\text{lock-in}}$, consistent with the resistivity result.

For the metallic $Y_5Ir_4Si_{10}$ sample, the measured magnetic susceptibility χ can be written as three temperature-independent terms

$$\chi = \chi^{\text{core}} + \chi^{\text{Pauli}} + \chi^{\text{Landau}}, \tag{1}$$

where χ^{core} is the core diamagnetism term, χ^{Pauli} is the Pauli paramagnetism due to the spin of conduction electrons, and χ^{Landau} is the diamagnetic orbital contribution due to conduction electrons. The core diamagnetism can be obtained by using the tabulated value of $\chi^{\text{core}}(Ir^{3+}) = -2.35 \times 10^{-4}$ (emu/mol).[25] The sum of Pauli paramagnetism and Landau diamagnetism can be expressed as

$$\chi^{\text{Pauli}} + \chi^{\text{Landau}} = \mu_0 \mu_B^2 \left[1 - \frac{1}{3}\left(\frac{m}{m^*}\right)^2 \right] N(\epsilon_F). \tag{2}$$

In the expression of Eq. (2), $\mu_0 = 4 \times 10^{-7}$(J/A^2 m) is the permeability, $\mu_B = 9.2741 \times 10^{-24}$(A m^2) is the Bohr magneton, m is the bare electron mass, m^* is the effective mass of conduction electron, and $N(\epsilon_F)$ is the density of states at the Fermi level in the unit of state/J mol. By converting the SI unit (m^3/mol) of molar magnetic susceptibility to the Gaussian unit (emu/mol), the molar magnetic susceptibility for $Y_5Ir_4Si_{10}$ can be written as follows

$$\chi = -2.35 \times 10^{-4} + 9.23 \times 10^{-4} \times \left[1 - \frac{1}{3}\left(\frac{m}{m^*}\right)^2 \right] N(\epsilon_F)(\text{emu/mol}), \tag{3}$$

where $N(\epsilon_F)$ is in the unit of state/eV atom. In the normal state, a value of $N(\epsilon_F) = 0.422$(state/eV atom) is estimated by using Eq. (3), which is reasonable for the metallic nature of $Y_5Ir_4Si_{10}$. Here we simply assume that the effective mass of conduction electron is equal to the bare electron mass. Note that the estimated $N(\epsilon_F)$ value represents an upper limit because m^* is usually larger than m. The occurrence of successive CDW transitions at T_{CDW1} and T_{CDW2} leads to a reduction of Pauli susceptibility by a value of 3×10^{-6}(emu/mol), corresponding to a change of density of states $\Delta N(\epsilon_F) \sim 0.005$(state/eV atom). Therefore, the CDW formation for the upper two transitions is responsible for a 1.2% of reduction in $N(\epsilon_F)$, i.e., the occurrence of these electronic phase transitions in $Y_5Ir_4Si_{10}$ results in an opening of energy gap over about 1.2% of the Fermi surface. It is worth mentioning that this value is independent of m/m^*, since the prefactor $\left[1 - \frac{1}{3}(m/m^*)^2\right]$ cancels out by taking the ratio of $\Delta N(\epsilon_F)$ and $N(\epsilon_F)$. Such an analysis suggests that the degree of Fermi surface nesting in $Y_5Ir_4Si_{10}$ is considerably weaker than that of its isostructural compound $Lu_5Ir_4Si_{10}$ (36% Fermi surface nesting),[3] and the phase transitions observed in $Y_5Ir_4Si_{10}$ could be described as a weak-coupled CDW system.

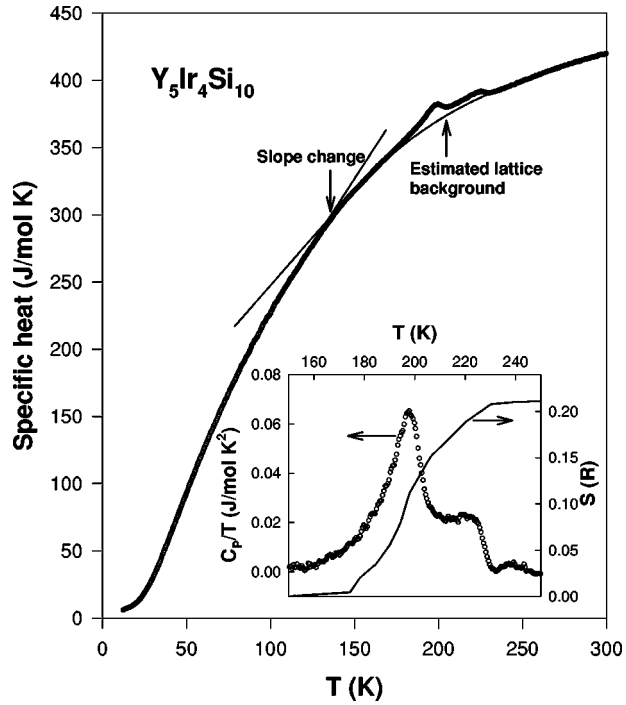

FIG. 5. The temperature (10–300 K) dependence of specific heat for $Y_5Ir_4Si_{10}$. The inset shows the plots of $\Delta C_p/T$ versus T and entropy change ΔS associated with the transitions.

D. Heat capacity

The temperature-dependent specific heat (C_P) for $Y_5Ir_4Si_{10}$ is illustrated in Fig. 5. Two pronounced peaks associated with the CDW formation are observed in C_P at $T_{CDW1} = 225$ K and $T_{CDW2} = 200$ K, respectively. The transition temperatures are determined from the temperature of the peak position. It is noted that the transition temperatures determined from C_P measurements are also consistent with the temperature-dependent resistivity result. No thermal hysteresis near the upper two transitions is found within the resolution limit of our apparatus. This is in contrast to that of its isostructural compound $Lu_5Rh_4Si_{10}$, in which pronounced thermal hysteresis loops between heating and cooling cycles have been observed in the vicinity of its CDW transition temperature $T_{CDW} \sim 147$ K.[20,26]

Previously we have successfully applied a least-squares fitting procedure to a model of critical fluctuations in addition to BCS mean-field contributions to the reported specific

heat data in the $R_5Ir_4Si_{10}$ compounds.[19,21] However, such an analysis seems to be inappropriate for the present case of $Y_5Ir_4Si_{10}$, because the two transitions overlap and it is difficult to deconvolute them without the exact model for their shapes. Nevertheless, the sharpness of the transition $\Delta T_{CDW}/T_{CDW}$, the excess specific heat $\Delta C_P/C_P$, and the entropy change ΔS near the transitions can be extracted from our measured data. The transition width ΔT_{CDW} was defined by the temperature width of half peak height. The specific heat jumps ΔC_P and entropy change ΔS near the transitions in $Y_5Ir_4Si_{10}$ can be estimated by subtracting a smooth lattice background fitted far away from the transition, drawn as a solid curve in Fig. 5. It is estimated that the sharpness of the transition $\Delta T_{CDW}/T_{CDW}$ is about 5% for both transitions at 225 and 200 K, and the excess specific heat $\Delta C_P/C_P$ is 1.2% at 225 K and 3.4% at 200 K for $Y_5Ir_4Si_{10}$. It is worth mentioning that the observed spike-shaped C_P anomalies in the $R_5Ir_4Si_{10}$ (R=Dy-Lu) series suggest that these compounds could be classified as the strong-coupled CDW systems, due to their short coherence length deduced from the Ginzburg criteria.[19,21] Accordingly, there are a large number of soft phonon modes in the transition region which provide a substantial heat capacity arising from their occupation. In contrast, the specific heat peaks for $Y_5Ir_4Si_{10}$ are relatively weaker than that of those observed in $R_5Ir_4Si_{10}$ (R =Dy to Lu), indicative of a weak-coupled CDW system for $Y_5Ir_4Si_{10}$. Besides, the entropy change ΔS=0.21 R near the transitions is calculated by integrating the area under the C_P/T versus T curve, as shown in the inset of Fig. 5. We notice that the estimated total entropy change in $Y_5Ir_4Si_{10}$ is compatible to that obtained for other $R_5Ir_4Si_{10}$ compounds,[19,21] even though the observed transitions in $Y_5Ir_4Si_{10}$ appear to be weaker. This is mainly because the influence of phase transitions affects a rather wide temperature range (~50 K), which in turn gives rise to an enhancement on the area (ΔS) under C_P/T versus T curve.

In addition to the well-defined peaks found near the upper two CDW transition temperatures, a weaker secondary C_P anomaly (slope change) was also detected in $Y_5Ir_4Si_{10}$ with our high-resolution calorimeter at $T_{lock\text{-}in}$=140 K, as demonstrated by the arrow in Fig. 4. A similar slope change in C_P was also observed in $Er_5Ir_4Si_{10}$ at 60 K.[19] Since the lock-in transition does not involve gap opening processes, consequently there is only very little amount of entropy change during the transition.

E. Thermal conductivity

The temperature-dependent thermal conductivity (κ) for $Y_5Ir_4Si_{10}$ is illustrated in Fig. 6. The value of room-temperature κ for $Y_5Ir_4Si_{10}$ is about 110 mW/cm K, reasonable for its metallic character. At low temperatures, κ increases with temperature, and then develops into a broad maximum at around 30 K. This is a typical feature for the reduction of thermal scattering at lower temperatures for solids. Anomalies were also found in κ at $T_{lock\text{-}in}$=140 K and T_{CDW2}=200 K. However, there is no noticeable anomaly in κ at T_{CDW1}=220 K. Due to the metallic nature of the sample, the total thermal conductivity κ_T can be expressed as a sum

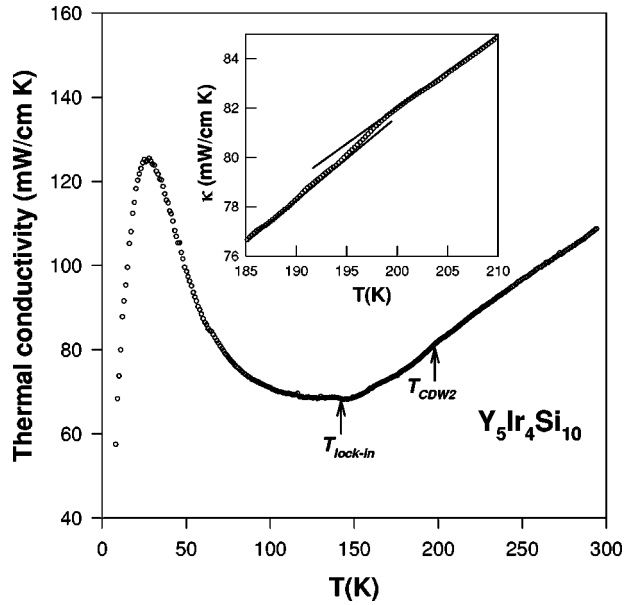

FIG. 6. Thermal conductivity versus temperature for $Y_5Ir_4Si_{10}$. Inset: a close-up plot near the phase transition at T_{CDW2}=200 K.

of lattice (κ_L), electronic (κ_e), and anomalous terms ($\Delta\kappa$): $\kappa_T=\kappa_L+\kappa_e+\Delta\kappa$. The lattice part κ_L is expected to follow $1/T$ behavior, while the electronic contribution κ_e can be determined by means of the Wiedmann-Franz law: $\kappa_e\rho/T=L_o$. Here ρ is the dc electrical resistivity and the Lorentz number $L_o=2.45\times10^{-8}$ W Ω K^{-2}. As suggested previously, the anomalous features in are essentially of electronic origin in $R_5Ir_4Si_{10}$ (R=Dy-Lu) series.[19,21] This scenario is also perfectly applicable for the present $Y_5Ir_4Si_{10}$ case, where a reduction in κ at 200 K and an increase at 140 K correspond well to the increase and reduction respectively in ρ at these phase transitions. Compared to the appearance of giant $\Delta\kappa$ generally observed at $T_{CDW's}$ for other members of $R_5Ir_4Si_{10}$, $Y_5Ir_4Si_{10}$ exhibits rather weak response in κ at phase transitions. Since anomalous peaks in κ were also observed in the strong-coupled $K_{0.3}MoO_3$ and $(TaSe_4)_2I$ at their CDW transitions,[27] the absence of the thermal conductivity peak for $Y_5Ir_4Si_{10}$ indicates that the titled material is a weak-coupled CDW system.

Another peculiar feature of the thermal conductivity in $Y_5Ir_4Si_{10}$ is the high-temperature variation. In the normal state ($T>T_{CDW1}$), the κ data increase monotonically with temperature. Such behavior has also been found in other CDW materials such as $K_{0.3}MoO_3$ and $(TaSe_4)_2I$, and it was attributed to the quasiparticle scattering due to fluctuations.[27] As a result, a large number of soft Kohn-Peierls phonons would contribute to the high-T thermal conductivity, which in turn gives a linear increase in κ at higher temperatures. In fact, the lack of this feature in the isostructural compound $Sc_5Ir_4Si_{10}$ (with no CDW transition) further supports that the linear increase in κ at higher temperatures for $Y_5Ir_4Si_{10}$ is related to CDW formation, arising from the quasiparticle excitations.[28]

F. Seebeck coefficient

The temperature-dependent thermoelectric power (TEP) of $Y_5Ir_4Si_{10}$ is shown in Fig. 7. As one can see that the

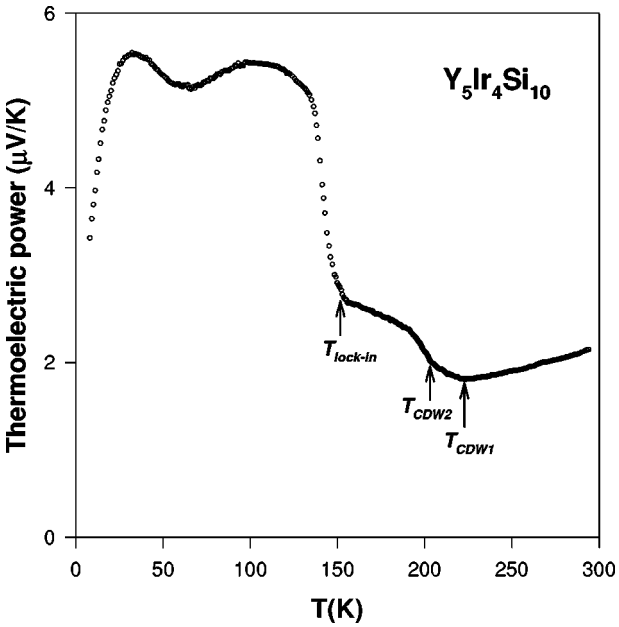

FIG. 7. Thermoelectric power as a function of temperature for $Y_5Ir_4Si_{10}$.

T-dependent TEP of $Y_5Ir_4Si_{10}$ exhibits the most anomalous features among all measured physical quantities. Such an observation indicates a very complicated heat transport process in $Y_5Ir_4Si_{10}$ during the CDW transitions. The values of TEP are positive for the whole temperature range we investigated, signifying that hole-type carriers dominate the thermoelectric transport in this material, consistent with the Hall measurement. Since TEP varies rather linearly with temperature in the normal state (above 220 K), one can try to extract the value of ϵ_F through the classical formula $S = \pi^2 k_B^2 T/2e\epsilon_F$, assuming a one-band model with an energy-independent relaxation time. A value of $\epsilon_F = 6.1$ eV was obtained from this simple model, in agreement with the metallic character of the sample. Three pronounced anomalies in TEP were discovered at $T_{\mathrm{CDW1}} = 220$ K, $T_{\mathrm{CDW2}} = 200$ K, and $T_{\text{lock-in}} = 140$ K, respectively, due to CDW formation. Upon further cooling, TEP exhibits a broad maximum at around 30 K, presumably due to the phonon-drag effect.

Since the TEP measurement is a sensitive probe of the density of states close to the Fermi surface, the rapid changes of TEP in $Y_5Ir_4Si_{10}$ are attributed to the sudden change of the band structure, associated with the electron-hole asymmetry at the transitions. Thus it would be instructive to compare the Hall coefficient data with the thermoelectric power data in this compound. Below $T_{\text{lock-in}} \sim 140$ K, the Hall coefficient of $Y_5Ir_4Si_{10}$ decreases sharply and then changes sign to negative at low temperature, while its thermoelectric powers remain positive at all temperatures. The difference in sign of dominant carriers at low temperatures as obtained from the Hall coefficient and thermoelectric power data suggests that $Y_5Ir_4Si_{10}$ has the comparable size of electron-pockets and hole-pockets in its energy band. For simplicity, we assume that the electron concentration n is equal to the hole concentration p, and the $Y_5Ir_4Si_{10}$ compound is fully compensated. Thus the thermoelectric power and Hall coefficient can be simply written as: $R_H = (1/ne)(\mu_h - \mu_e)/(\mu_h + \mu_e)$, $S = (\mu_h S_h - \mu_e S_e)/(\mu_h + \mu_e)$, where μ_h and μ_e are the mobilities of the holes and electrons, respectively. From this simple model, a drastic change in the electronic mobility below $T_{\text{lock-in}}$ would account for the sign difference in the low-temperature thermoelectric power and Hall coefficient data of $Y_5Ir_4Si_{10}$.

IV. CONCLUSIONS

In conclusion, we have presented the results of electrical resistivity (ρ), Hall coefficient (R_H), specific heat (C_P), magnetic susceptibility (χ), thermal conductivity (κ), as well as thermoelectric power (TEP) on the rare-earth-transition-metal compound $Y_5Ir_4Si_{10}$ as a function of temperature. For all measured physical properties, successive anomalies due to charge-density-wave (CDW) formation were observed. In contrast to its isostructural compounds $R_5Ir_4Si_{10}$ (R = Dy, Ho, Er, Tm, and Lu) found to be strong-coupled CDW materials, $Y_5Ir_4Si_{10}$ exhibits relatively weak anomalous responses for all measured physical quantities. Such an observation suggests that $Y_5Ir_4Si_{10}$ could be classified as a weak-coupled CDW system, and the electronic-configuration difference also significantly affects the physical properties in this class of materials. Most intriguingly, the complex temperature-dependent thermoelectric power and sign reversal of the Hall coefficient in this compound indicate a drastic modification of the band structure near its Fermi surface or a drastic change in the electronic mobility at these transitions. Apparently, the transition features in $Y_5Ir_4Si_{10}$ are unique and deserve further studies. Especially, single crystal x-ray diffraction or neutron scattering measurements are needed to understand the microscopic nature of these phase transitions.

ACKNOWLEDGMENTS

This work was supported by the National Science Council, Taiwan, under Grant Nos. NSC-92-2112-M-259-011 (Y.K.K.), NSC-92-2112-M-212-001 (L.M.W.), and NSC-92-2112-M-110-017 (H.D.Y.).

*Electronic address: ykkuo@mail.ndhu.edu.tw
†Electronic address: yang@mail.phys.nsysu.edu.tw

[1] For an extensive review article: A. M. Gabovich and A. I. Voitenko, Low Temp. Phys. **26**, 305 (2000).
[2] H. D. Yang, R. N. Shelton, and H. F. Braun, Phys. Rev. B **33**, 5062 (1986).
[3] R. N. Shelton, L. S. Hausermann-Berg, P. Klavins, H. D. Yang, M. S. Anderson, and C. A. Swenson, Phys. Rev. B **34**, 4590 (1986).
[4] L. S. Hausermann-Berg and R. N. Shelton, Phys. Rev. B **35**, 6659

(1987).
[5] P. J. Chu, B. C. Gerstein, H. D. Yang, and R. N. Shelton, Phys. Rev. B **37**, 1796 (1988).
[6] C. A. Swenson, R. N. Shelton, P. Klavins and H. D. Yang, Phys. Rev. B **43**, 7668 (1991).
[7] H. D. Yang, P. Klavins, and R. N. Shelton, Phys. Rev. B **43**, 7676 (1991).
[8] H. D. Yang, P. Klavins, and R. N. Shelton, Phys. Rev. B **43**, 7681 (1991).
[9] H. D. Yang, P. Klavins, and R. N. Shelton, Phys. Rev. B **43**, 7688 (1991).
[10] S. Ramakrishnan, K. Ghosh, and Girish Chandra, Phys. Rev. B **45**, 10 769 (1992).
[11] S. Ramakrishnan, K. Ghosh, and Girish Chandra, Phys. Rev. B **46**, 2958 (1992).
[12] K. Ghosh, S. Ramakrishnan, and Girish Chandra, Phys. Rev. B **48**, 4152 (1993).
[13] S. Ramakrishnan, K. Ghosh, Arvind D. Chinchure, Kristian Jonason, V. R. Marathe, and Girish Chandra, Phys. Rev. B **51**, 8398 (1995).
[14] M. H. Jung, H. C. Kim, A. Migliori, F. Galli, and J. A. Mydosh, Phys. Rev. B **68**, 132102 (2003).
[15] B. Becker, N. G. Patil, S. Ramakrishnan, A. A. Menovsky, G. J. Nieuwenhuys, J. A. Mydosh, M. Kohgi, and K. Iwasa, Phys. Rev. B **59**, 7266 (1999).
[16] F. Galli, S. Ramakrishnan, T. Taniguchi, G. J. Nieuwenhuys, J. A. Mydosh, S. Geupel, J. Ludecke, and S. van Smaalen, Phys. Rev. Lett. **85**, 158 (2000).
[17] F. Galli, R. Feyerherm, R. Hendrikx, S. Ramakrishnan, G. J. Nieuwenhuys, and J. A. Mydosh, Phys. Rev. B **62**, 13 840 (2000).
[18] S. van Smaalen, M. Shaz, L. Palatinus, P. Daniels, F. Galli, G. J. Nieuwenhuys, and J. A. Mydosh, Phys. Rev. B **69**, 014103 (2004).
[19] Y. K. Kuo, F. H. Hsu, H. H. Li, H. F. Huang, C. W. Huang, C. S. Lue, and H. D. Yang, Phys. Rev. B **67**, 195101 (2003).
[20] C. S. Lue, Y. K. Kuo, F. H. Hsu, H. H. Li, and H. D. Yang, P. S. Fodor and L. E. Wenger, Phys. Rev. B **66**, 033101 (2002).
[21] Y. K. Kuo, C. S. Lue, F. H. Hsu, H. H. Li, and H. D. Yang, Phys. Rev. B **64**, 125124 (2001).
[22] S. Drouard, D. Groult, J. Dumas, R. Buder, and C. Schlenker, Eur. Phys. J. B **16**, 593 (2000).
[23] R. Bel, K. Behnia, and H. Berger, Phys. Rev. Lett. **91**, 066602 (2003).
[24] N. P. Ong, Phys. Rev. B **18**, 5272 (1978).
[25] P. W. Selwood, *Magnetochemistry*, 2nd ed. (Interscience, New York, 1956), p. 78.
[26] C. S. Lue, F. H. Hsu, H. H. Li, H. D. Yang, and Y. K. Kuo, Physica C **364-365**, 243 (2001).
[27] R. S. Kwok and S. E. Brown, Phys. Rev. Lett. **63**, 895 (1989).
[28] Y. K. Kuo, Y. -T. Pan, C. S. Lue, and H. D. Yang, J. Low Temp. Phys. **131**, 311 (2003).